Volume 11
Number 12
28 March 2023
Pages 3893–4256

Journal of Materials Chemistry C

Materials for optical, magnetic and electronic devices

rsc.li/materials-c

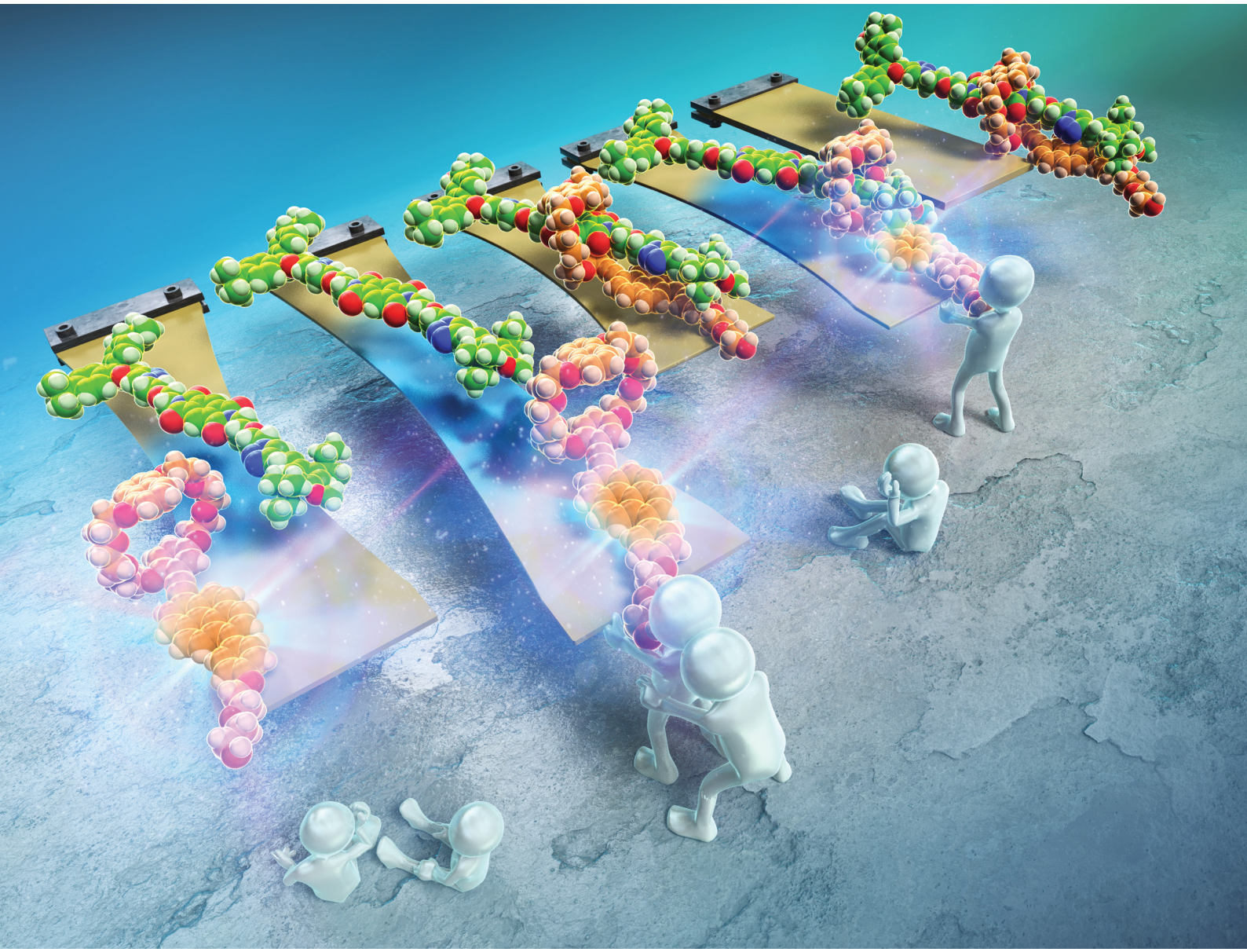

ISSN 2050-7526

ROYAL SOCIETY OF CHEMISTRY

PAPER

Go Watanabe, Yoshimitsu Sagara *et al.*
Tuning the mechanoresponsive luminescence of rotaxane mechanophores by varying the stopper size

10 YEARS ANNIVERSARY

Journal of Materials Chemistry C

ROYAL SOCIETY OF CHEMISTRY

PAPER

View Article Online
View Journal | View Issue

Cite this: J. Mater. Chem. C, 2023, 11, 3949

Tuning the mechanoresponsive luminescence of rotaxane mechanophores by varying the stopper size†

Keiko Hiratsuka,[a] Tatsuya Muramatsu,[a] Takuya Seki,[b] Christoph Weder,[c] Go Watanabe *[bd] and Yoshimitsu Sagara *[ae]

Mechanochromic mechanophores are useful molecular mechano-probes that can visualize forces in polymeric materials. Here, we report detailed studies on the correlation between the mechanoresponsive luminescent behaviour of rotaxane mechanophores and the size of the stopper used in the mechanophores. Five different stoppers were introduced at one end of the axle molecule, which featured an electron-deficient quencher group at its center. The same ring molecule carrying an electron-rich fluorophore was used in all rotaxanes. In solution, the blue fluorescence of the emitter is almost completely quenched for all rotaxanes, on account of charge-transfer interactions between the fluorophore and quencher. The mechanoresponsive character of these motifs was investigated by incorporating them into linear segmented polyurethanes (PUs). Sufficiently bulky stoppers prevent the ring of rotaxane from dethreading, and this leads to a fully reversible change of the emission intensity when films of the rotaxane-containing PUs are stretched and relaxed. This response is caused by the force-induced shuttling of the emitter-containing cycle away from and back to the quencher, without any breakage of the interlocked structure or dethreading. By contrast, small stoppers allow the rings to dethread from the axles of the rotaxanes, and the fluorescence turn-on triggered by deformation becomes fully or partially irreversible. In this case, the fraction of dethreaded rings and the residual fluorescence intensity gradually increases as samples are repeatedly strained. Molecular dynamics simulations show that the energy required for dethreading depends strongly on the size of the stopper, and confirm our experimental observations. Our data show that the response of rotaxane mechanophores can be easily varied between fully reversible and irreversible, and this allows one to create polymers with a broad range of mechanoresponsive luminescence behaviours.

Received 27th January 2023,
Accepted 16th February 2023

DOI: 10.1039/d3tc00330b

rsc.li/materials-c

Introduction

Mechanochromic mechanophores, which change their optical absorption and/or photoluminescence (PL) when a mechanical force is applied, are receiving attention because of their potential use as reporters that can visualize stresses and strains in polymers.[1–3] Since spiropyran was reported as the first mechanochromic mechanophore in 2009,[4] a variety of mechanophores have been reported to show mechanochromic effects that are rooted in the scission of covalent bonds.[5–33] Some mechanochromic mechanophores which need scission of covalent bonds for activation require time or additional energy such as light irradiation or thermal treatment to recover initial molecular structures,[6–9,11–16] except for a few mechanophores.[33] The other mechanochromic mechanophores that rely on breakage of covalent bonds are inherently irreversible.[21–31] Therefore, such mechanophores would be used as mechanoprobes to assess past (cumulative) force effects. The investigation of instantaneous effects requires mechanophores that change their photophysical properties instantly and reversibly. For such purposes, mechanophores that function without covalent bond scission and instantly revert back to their original state when the force is removed are preferable.[34–56] Supramolecular mechanophores in which the assembly of multiple chromophores, luminophores,

[a] Department of Materials Science and Engineering, Tokyo Institute of Technology, 2-12-1 Ookayama, Meguro-ku, Tokyo 152-8552, Japan. E-mail: sagara.y.aa@m.titech.ac.jp
[b] Department of Physics, School of Science, Kitasato University, 1-15-1 Kitasato, Minami-ku, Sagamihara, Kanagawa 252-0373, Japan. E-mail: go0325@kitasato-u.ac.jp
[c] Adolphe Merkle Institute, University of Fribourg, Chemin des Verdiers 4, CH-1700, Fribourg, Switzerland
[d] Kanagawa Institute of Industrial Science and Technology (KISTEC), 705–1 Shimoizumi, Ebina, Kanagawa 243–0435, Japan
[e] Living Systems Materialogy (LiSM) Research Group, International Research Frontiers Initiative (IRFI), Tokyo Institute of Technology 4259 Nagatsuta-cho, Midori-ku, Yokohama 226-8501, Japan

† Electronic supplementary information (ESI) available. See DOI: https://doi.org/10.1039/d3tc00330b

and/or quenchers and therewith the optical properties can be mechanically altered have been shown useful in this context.[2] Rotaxanes,[34–38] cyclophanes,[39,40] and loop-forming motifs[41–43] have been demonstrated to reversibly change their PL properties in response to mechanical force. While the De Bo group reported force-induced breakages of covalent bonds in several rotaxanes,[57,58] we demonstrated that the molecular shuttling effect in rotaxanes can be exploited to achieve reversible mechanoresponsive luminescence without any covalent bond scission.[34–37] Our previously reported rotaxane mechanophores are composed of a cyclic molecule with an appended luminophore and a rod-like axle molecule containing a matching quencher in the middle and two stoppers at both ends. The quencher and the cycle show weak charge transfer interactions, which in the force-free state causes the formation of an inclusion complex and quenching of the luminophore. Photo-induced electron transfer (PET) would also contribute to the quenching. When a sufficiently large mechanical force is applied through polymers attached to the cycle and the axle, the cycle slides along the axle, and the ensuing spatial separation between the quencher and the luminophore limits their electronic interactions or PET. Therefore, strong PL was observed when films of elastic polymers in which the mechanophores were covalently embedded were uniaxially deformed.[35–37] Upon removal of the force, the films contract and the emission is instantly quenched again. The response is reversible over many stretch and release cycles when rotaxanes are used that contain tetraphenylmethane units equipped with three *tert*-butyl groups as stoppers, suggesting that mechanically induced dethreading does not occur.[35–37] However, when a rotaxane mechanophore with a 1,4-di-*tert*-butylbenzene stopper was employed, reversible as well as irreversible changes of the PL intensity were observed. The latter irreversible behaviour is caused by force-induced dethreading.[34]

Here we demonstrate that the efficiency of force-induced dethreading of rotaxane mechanophores can be controlled by the stopper size and that this allows one to create polymers with a broad range of mechanoresponsive luminescence behaviours. Although force-induced dethreading of rotaxanes has been already reported by several groups,[59–61] this effect was primarily studied by molecular force spectroscopy and no systematic investigations of how the molecular structures of the stopper groups affect the dethreading have been carried out. Here we combine molecular dynamics simulations, which represent a useful tool for revealing the dynamics of the rotaxanes at the atomic level,[62,63] with *in situ* PL measurements of rotaxane-containing PUs to show that the dethreading efficiency scale with the size of the stoppers. We demonstrate that judicious choice of stoppers can be used to tailor the response of rotaxane mechanophores between fully reversible and irreversible (Fig. 1).

Results and discussion

We designed and synthesized a series of rotaxanes (**Rot1-5**) in which the chemical structure of the stopper facing the end of the rod molecule towards which the cyclic molecule is drawn upon application of force changes (Fig. 2). Bis(4-*tert*-butylphenyl) methane, bis(4-methylphenyl)methane, diphenylmethane, 1,4-di-*tert*-pentylbenzene, and 1,4-di-*tert*-butylbenzene groups were incorporated in **Rot1**, **Rot2**, **Rot3**, **Rot4**, and **Rot5**, respectively. In all rotaxanes, the same diphenylmethane-based stopper featuring one *tert*-butyl and one 1-hydroxy-2-methylpropyl group was used to cap the second end of the axle molecule. Hydroxy groups connected to the common stopper and to the cycle-appended luminophore were used to covalently incorporate the mechanophores into polymer backbones, which can transfer mechanical forces to these sites (Fig. 2). A pyromellitic diimide (PMDI) was embedded as a quencher in the center of the axle molecule and a blue-light emitting 1-phenyl-6-(phenylethynyl)-pyrene, which differs from the 9,10-(phenylethynyl)anthracene used in previous experiments,[34] formed part of the cycle. The

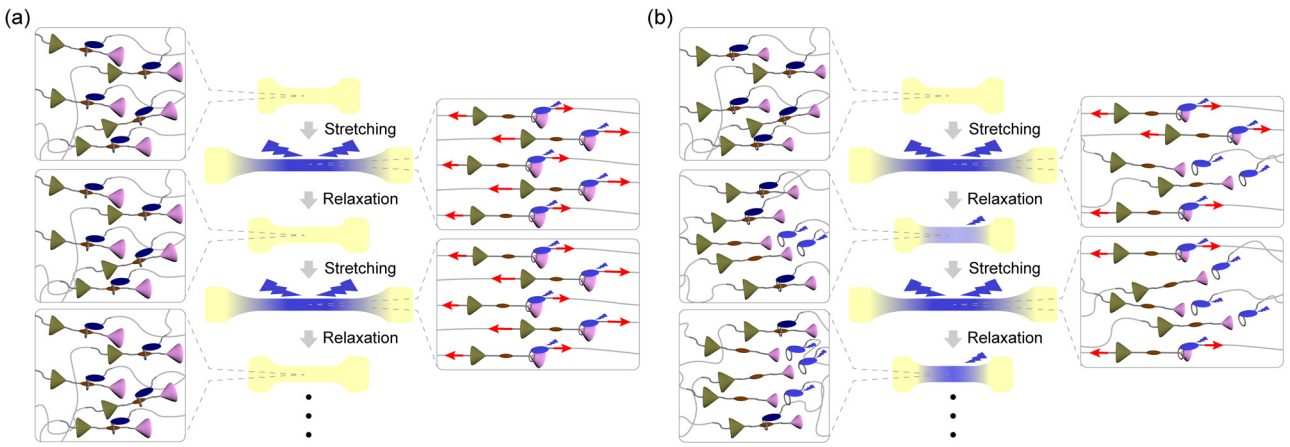

Fig. 1 Schematic illustrations of mechanoresponsive luminescence exhibited by rotaxane mechanophore equipped with (a) sufficient bulky stoppers and (b) small stoppers in polyurethane films. In the initial state, the quencher (brown) is intercalated by the ring featuring luminophore (blue). When the films in panel (a) are stretched, bulky stoppers (pink) fully prevent the rings from dethreading. In the case of panel (b), some rings can pass the smaller stopper (pink). The number of dethreaded rings increases with the number of stretch and release cycles.

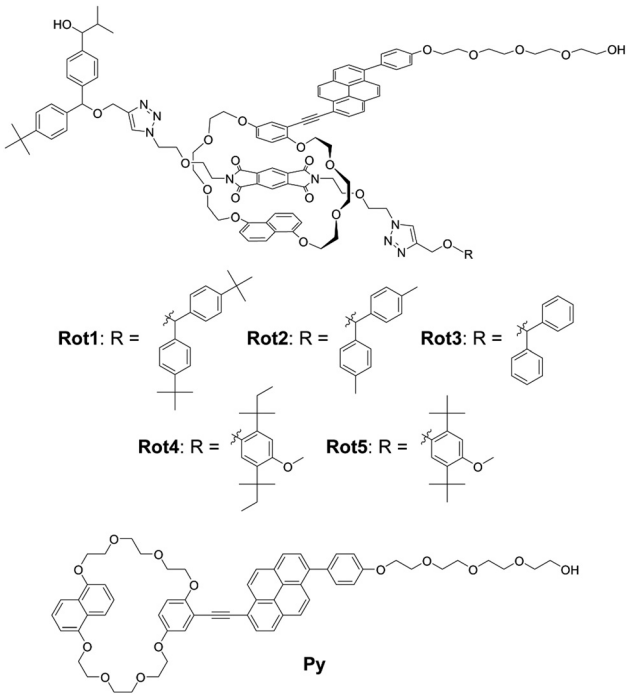

Fig. 2 Chemical structures of rotaxane-based supramolecular mechanophores **Rot1-5** and ring reference **Py**.

current emitter was chosen because 1,6-disubstituted pyrene derivatives show high quantum efficiency.[64–66] Besides, the PMDI and pyrene groups have been reported to form charge transfer (CT) complexes.[67,68] The luminophore was appended with a tetraethyleneglycol chain in order to improve the solubility of the cyclic building block. This aspect is important for the yield of the Cu(I)-catalyzed Huisgen click reactions[69,70] between the axle molecule featuring a terminal alkyne and the azide group-containing stoppers, which were used for the rotaxane synthesis. This reaction requires a high concentration of all components for the pseudo rotaxane formation to be efficient (ESI†). Yields of 3–17% were attained for this step, and all rotaxanes were fully characterized by ^{1}H and ^{13}C NMR spectroscopy and high-resolution electrospray ionization mass spectrometry (ESI†). In each case, the ^{1}H NMR spectra display diagnostic shifts of the peaks corresponding to the aromatic protons that confirm the rotaxane formation (Fig. S1, ESI†). Ring molecule **Py** was synthesized as a reference compound.

The UV-vis absorption and PL spectra of all rotaxanes and reference **Py** were first measured in chloroform ($c = 1.0 \times 10^{-5}$ M) (Fig. 3 and Fig. S2, ESI†). The absorption spectrum of **Py** shows an absorption band with peaks at 388 and 407 nm and another sharp peak at 296 nm (Fig. 3a). The PL spectrum has peaks at 430 and 449 nm (Fig. 3b) and the PL quantum yield $\Phi = 0.85$ is high. These spectral features are comparable to those of a reported 1-phenyl-6-(phenylethynyl)pyrene derivative.[35] The absorption spectra of rotaxanes **Rot1-5** display similar peaks as **Py**, but in each case the absorption spectrum shows a tail towards longer wavelengths, which is ascribed to CT complex formation between the luminophore and PMDI. In all rotaxanes, the fluorescence of the emitter

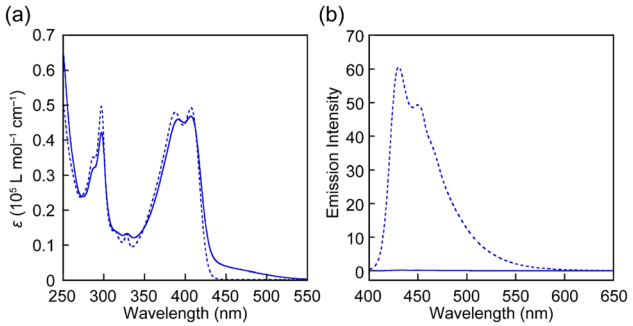

Fig. 3 (a) UV-vis absorption and (b) PL spectra of **Rot-1** (solid line) and **Py** (dotted line) in chloroform ($c = 1.0 \times 10^{-5}$ M). The excitation wavelength was 380 nm.

is completely quenched. As expected, the absorption and emission spectra of all rotaxanes are practically identical, *i.e.*, the nature of the stopper does not affect the photophysical properties in the force-free state in the solution.

Rot1-5 were separately incorporated into linear segmented polyurethanes (PUs) to investigate the mechanoresponsive luminescence. The specific composition was selected as it shows high elasticity and extensibility and is thus suitable to probe the response of supramolecular mechanophores.[34–37,39–42] Moreover, the same PU platform was used in previous studies,[34–37,39–41] which makes it possible to evaluate and compare the mechanoresponsive behaviour of the motifs investigated here with other mechanophores. To enable a direct comparison of the mechanoresponses, polymers of otherwise identical composition and similar number-averaged molecular weights (M_n) were made and processed under identical conditions (see below and ESI†). The PUs were synthesized through dibutyltin dilaurate catalyzed polyaddition reactions between the respective rotaxane ($\approx$ 0.002 wt%), telechelic poly(tetrahydrofuran)diol ($M_n \approx$ 2000 g mol^{-1}), 1,4-butanediol, and 4,4′-methylenebis(phenylisocyanate), which were carried out in THF and at room temperature (r.t.). The M_n of the resulting polymers **Rot1-PU**, **Rot2-PU**, **Rot3-PU**, **Rot4-PU**, and **Rot5-PU** ranges from 116 kg mol^{-1} to 139 kg mol^{-1}. The ^{1}H NMR spectra of these polymers display peaks that are characteristic of the polyurethanes, but no signals corresponding to rotaxane are discernible due to their low concentration (Fig. S3, ESI†). However, their incorporation was confirmed by UV-vis absorption spectra in DMF solutions, which display similar absorption bands as the rotaxanes in chloroform (Fig. S4, ESI†). The PL of the blue emitter remains quenched in DMF solutions of **Rot1-PU**, **Rot2-PU**, **Rot4-PU**, and **Rot5-PU** (Fig. S4, ESI†). By contrast, the solution of **Rot3-PU** exhibits blue PL that is derived from the emitter. We ascribe this to the fact that the **Py** ring gradually passes the diphenylmethane stopper. To probe under which conditions **Py** can dethread from the different rotaxanes in solution, the fluorescence intensities of **Rot1** and **Rot3** solutions in toluene were examined before and after heating the solutions for 3 h at 90 °C (Fig. 4). In the case of **Rot1** both solutions displayed almost no fluorescence and heating had practically no effect. By contrast, the fluorescence intensity of the **Rot3** solution significantly increased upon heating, due to heat-

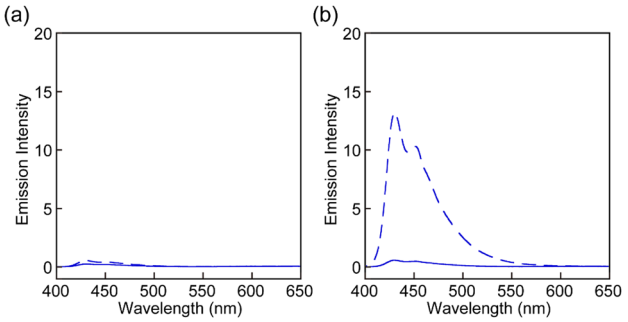

Fig. 4 PL spectra of the toluene solution of (a) **Rot1** and (b) **Rot3** before (solid lines) and after (dashed lines) heating for 3 h at 90 °C. The concentration of the solutions did not change upon heating. The PL spectra were recorded with the excitation light of 380 nm at r.t.

induced dethreading. HPLC analysis confirmed this effect, revealing the formation of free **Py** (Fig. S5, ESI†). Experiments with **Rot3** solutions in THF show that dethreading also occurs at r.t. for this rotaxane, although the process is much slower than at 90 °C (Fig. S6, ESI†).

Thin films of **Rot1-PU**, **Rot2-PU**, **Rot3-PU**, **Rot4-PU**, and **Rot5-PU** were prepared by solution-casting from THF (ESI†). As expected, the different polymers display almost identical mechanical and thermal properties (Fig. S7–S10 and Table S1, ESI†). The tensile tests (Fig. S7, ESI†) reveal Young's moduli of 10–13 MPa, a strain at break of *ca.* 700%, and a stress at break of 44–70 MPa. Dynamic mechanical analysis shows that all polymers display a rubbery regime from –10 to 150 °C (Fig. S8, ESI†). Furthermore, the dynamic scanning calorimetry and thermogravimetric analysis traces are also similar to each other (Fig. S9 and S10, ESI†). The differences shown between experiments are statistically insignificant (Table S1, ESI†) and appear to be caused by sample-to-sample variations, and not the mechanophore type. The properties are also similar to previously reported linear segmented polyurethanes,[34–37,39,40] suggesting that the incorporation of the rotaxanes with very low concentrations does not lead to specific "sliding ring" effects.

The mechanoresponsive PL of films of all polymers was investigated by *in situ* PL spectroscopy measurements that were combined with multi-cycle tensile tests. Before stretching, the **Rot1-PU**, **Rot2-PU**, **Rot4-PU**, and **Rot5-PU** films show very weak

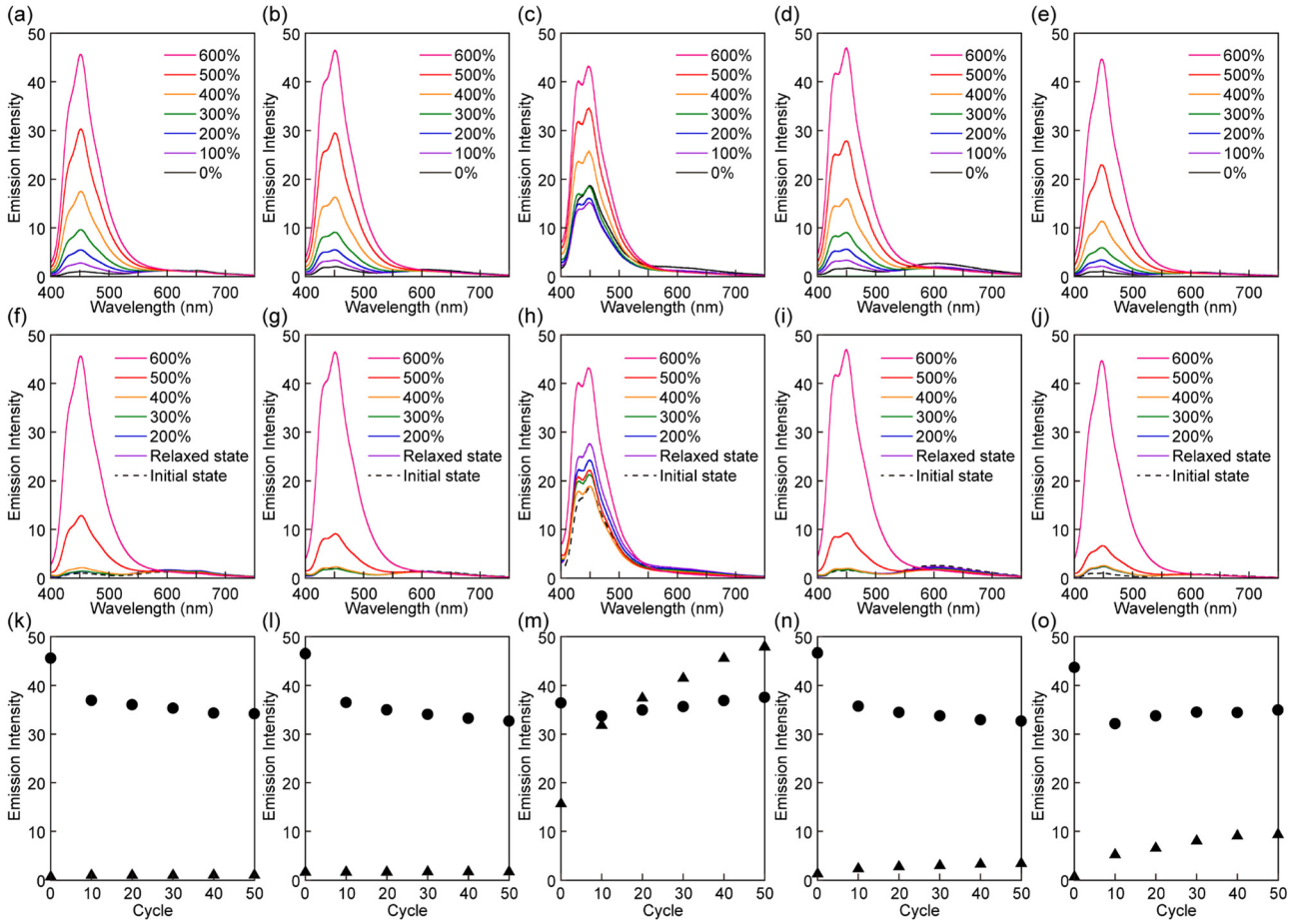

Fig. 5 Mechanoresponsive PL of films of **Rot1-PU** (a, f and k), **Rot2-PU** (b, g and l), **Rot3-PU** (c, h and m), **Rot4-PU** (d, i and n), and **Rot5-PU** (e, j and o). The top and middle panels show change in PL spectra upon the first stretching (top) and relaxation (middle) cycle. All spectra were recorded at the indicated strain. The bottom panels represent plots of the emission intensity at 450 nm recorded in cyclic tensile tests at strains of 600% (circles) and in the force-free state (triangles). All PL data were recorded with excitation at 380 nm.

blue emission from the luminophore (Fig. 5). The absence of any correlation between stopper size and intensity suggests that the emission is caused by mechanophores that were trapped in the activated state during processing.[39,40] The PL spectra of these films also display a faint emission band between 520 and 700 nm, which is ascribed to emission from a CT complex between the luminophore and the quencher. This is supported by the fact that a cyclophane-based mechanophore containing a pair of 1,6-bis(phenylethynyl)pyrene and PMDI exhibits CT complex emission at a similar wavelength.[40] Unlike the other polymers, the pristine **Rot3-PU** films show strong PL that is clearly associated with the luminophore, reflecting considerable dethreading of **Py** during the solvent casting process.

When the **Rot1-PU**, **Rot2-PU**, **Rot4-PU**, and **Rot5-PU** films were uniaxially stretched, the intensity of the emission from the blue emitter gradually increased with the applied stress (Fig. 5a, b, d, and e). For example, the emission intensity of the **Rot1-PU** film at 449 nm at a strain of 600% is 45 times higher than that before deformation, and similar responses were recorded for the other materials. Upon releasing the applied force, the original, little-emissive states are recovered (Fig. 5f, g, i, and j). The significant, reversible change in the emission intensity observed in the first stretch and release cycle appears to be largely driven by the force-induced shuttling function of the rotaxanes, whereas dethreading events that would cause irreversible changes appear to be rare. The **Rot3-PU** films also show an incremental increase of the monomer emission upon elongation after an initial decrease up to an elongation of 100% (Fig. 5c). The initial decremental effect is ascribed to decrease of excited luminophores in the irradiated area due to film-thinning upon stretching. Since the initial emission intensity of the **Rot3-PU** films is already quite pronounced, the emission contrast observed upon deformation is much lower than in the case of the other films. Furthermore, the emission intensity of the **Rot3-PU** films after the first stretch and relax cycle is higher than that before stretching (Fig. 5h). Thus, only one single elongation is sufficient to induce dethreading of a significant fraction of the rotaxane mechanophores, reflecting that the **Py** cycle can easily slip past the diphenylmethane stopper used in **Rot3**, as seen in the thermal experiments.

Further cyclic tensile tests reveal that dethreading is also possible in some of the other rotaxanes and revealed differences between rotaxanes **Rot1**, **Rot2**, **Rot4** and **Rot5**. Plots showing the fluorescence intensity at 450 nm of all films in the stretched state at a strain of 600% and in the relaxed state over 50 stretch and release cycles are shown in Fig. 5k, l, n and o. In all films, the intensity observed in the stretched state *drops* in the first few cycles, due to irreversible changes in the domain structure of segmented PUs upon stretching. No increase in emission intensity was measured under relaxed conditions for the **Rot1-PU** and **Rot2-PU** films over 50 stretching cycles, which indicates that under the mechanical conditions applied, the **Py** ring cannot slide past the bis(4-*tert*-butylphenyl)methane and bis(4-methylphenyl)methane stoppers. Thus, rotaxanes **Rot1** and **Rot2** can be considered as fully reversible supramolecular mechanophores that show only reversible PL changes. By contrast, the **Rot4-PU** and **Rot5-PU** films exhibit a gradual increase in monomer emission intensity as the number of deformation cycles increases, reflecting that the fraction of dethreaded **Py** rings increases with each cycle stretching. A comparison of the data (Fig. 5n and o) reflects that the ring can more easily pass the 1,4-di-*tert*-butylbenzene than the 1,4-di-*tert*-pentylbenzene stopper, as the relative residual PL intensity of the **Rot5-PU** films after 50 cycles is about 2.4 times as high as that of **Rot4-PU** films. Thus, the two additional methyl groups in 1,4-di-*tert*-pentylbenzene considerably reduce the dethreading efficiency. The data collected in the cyclic tensile tests clarified that the mechanoresponsive PL responses of **Rot4-PU** and **Rot5-PU** films also show a large reversible component, and therefore rotaxanes **Rot4** and **Rot5** can be considered as dual-type supramolecular mechanophores.[34] A much more dramatic increase of the PL emission intensity in the relaxed state was observed for the **Rot3-PU** films (Fig. 5m), in which case differences between the relaxed and the stretched state disappear after only a few cycles. Thus, **Rot3** is an extremely sensitive mechanophore that shows irreversible PL changes at presumably extremely low forces.

To correlate the force-induced dethreading of the ring from the rotaxane with the size of the stopper were also confirmed by MD simulations performed for **Rot1**, **Rot3**, and **Rot4**. The MD simulations of the rotaxanes in diethyl ether (DEE) without any restraints and external forces show that **Rot1**, **Rot3**, and **Rot4** are thermally stable so that the ring molecule cannot slide past these stoppers at 300 K (see Movies S1–S3, ESI†).

The steered MD simulations (Fig. 6) were also performed for exploring the possible pathway of the ring molecule being pulled away from the axle molecule by applying an external force (see Movies S4–S6, ESI†). Since the axle molecule was pulled at a constant velocity in the steered MD simulations of this study, the time dependence of the external pulling force can be investigated as shown in Fig. S11 (ESI†). The pulling forces increase linearly until the ring molecule is about to pass through the stopper of the rod molecule. Beyond this point, the values of the pulling force rapidly decrease to zero. The maximum values of the time-dependent pulling force are 2.71×10^3 kJ mol^{-1} nm^{-1} at 9.2 ns for **Rot1**, 9.61×10^2 kJ mol^{-1} nm^{-1} at 6.6 ns for **Rot3**, and 1.38×10^3 kJ mol^{-1} nm^{-1} at 7.3 ns for **Rot4**. The data indicates that the external force required to pull the ring molecule away from the rotaxane decreases in the order **Rot1** > **Rot4** > **Rot3**.

For a more quantitative discussion, the free energy barriers for dethreading of the rotaxanes were estimated using the potential of mean force (PMF). As shown in Fig. 6b, the PMFs for pulling the ring molecule of the rotaxane past the stopper are 195 ± 10 kJ mol^{-1} for **Rot1**, 71 ± 19 kJ mol^{-1} for **Rot3**, and 101 ± 29 kJ mol^{-1} for **Rot4**. Since the thermal energy of 2 molecules at 300 K can be estimated about 5 kJ mol^{-1}, all the rotaxanes simulated were energetically stable. While the PMF values for **Rot1** and **Rot4** correspond to the maximum, that for **Rot3** was obtained from the difference between the minimum and maximum. This is because the initial structure of the first umbrella sampling simulation might be not the thermally most

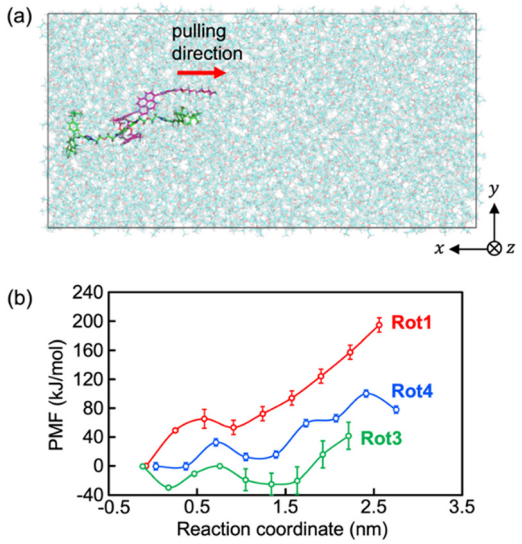

Fig. 6 (a) Steered MD simulation snapshot of **Rot1** in the initial state. The ring and axle molecules are shown as purple and green sticks, respectively. Surrounding thin sticks in cyan represent DEE. (b) Potential of mean force (PMF) profiles of **Rot1**, **Rot3**, and **Rot4**. The error bars depict only the statistical uncertainty from the connection of probability density by the weighted histogram method.

stable. The analysis of the PMF shows that it is required more energy and pulling force for dethreading of the rotaxanes of which the stopper of the rod molecule is larger or bulkier.

Conclusions

In conclusion, we demonstrated that force-induced dethreading of the ring of rotaxane from the rod group depends on the stopper bulkiness. Whether the dethreading occurs or not determines the mechanoresponsive luminescence of the rotaxane mechanophores. Our experimental and MD simulations results show clearly a correlation between the threading efficiency and the bulkiness of the stopper. The two large stoppers, bis(4-*tert*-butylphenyl)methane (**Rot1**) and bis(4-methylphenyl)methane (**Rot2**), completely prevent dethreading at the forces that the mechanophores experience upon deformation of polyurethane films. By contrast, the ring can easily slide past the diphenylmethane group (**Rot3**). The 1,4-di-substituted benzene-based stoppers show an intermediate behaviour. Intriguingly, the resistance to dethreading is extremely sensitive to the nature of auxiliary substituents attached to the benzene moieties. For example, changing the design from *tert*-pentyl (**Rot4**) to *tert*-butyl (**Rot5**) groups considerably affects the capability for dethreading. Our data show that the response of rotaxane mechanophores can be easily varied between fully reversible and irreversible, and this allows one to create polymers with a broad range of mechanoresponsive luminescence behaviours.

Conflicts of interest

There are no conflicts to declare.

Acknowledgements

We thank Mr Masato Koizumi at Open Facility Center, Tokyo Institute of Technology for HRMS measurements. This work was partially supported by Japan Science Technology Agency (JST), PRESTO (No. JPMJPR17P6) and FOREST (No. JPMJFR201N). This work was partially supported by JSPS KAKENHI (grant no. JP18H02024, JP19H02537, JP19H05718, JP20H05198, and JP 22H04531). Financial support through the National Center of Competence in Research (NCCR) Bio-Inspired Materials, a research instrument of the Swiss National Science Foundation (SNF) as well as funding from the Adolphe Merkle Foundation is gratefully acknowledged. The computations were partially performed at the Research Center for Computational Science, Okazaki, Japan (Project: 21-IMS-C043, 22-IMS-C043).

Notes and references

1 Y. Chen, G. Mellot, D. Van Luijk, C. Creton and R. P. Sijbesma, *Chem. Soc. Rev.*, 2021, **50**, 4100–4140.
2 H. Traeger, D. J. Kiebala, C. Weder and S. Schrettl, *Macromol. Rapid Commun.*, 2021, 2000573.
3 S. He, M. Stratigaki, S. P. Centeno, A. Dreuw and R. Göstl, *Chem. - Eur. J.*, 2021, **27**, 15889–15897.
4 D. A. Davis, A. Hamilton, J. Yang, L. D. Cremar, D. Van Gough, S. L. Potisek, M. T. Ong, P. V. Braun, T. J. Martinez, S. R. White, J. S. Moore and N. R. Sottos, *Nature*, 2009, **459**, 68–72.
5 M. J. Robb, T. A. Kim, A. J. Halmes, S. R. White, N. R. Sottos and J. S. Moore, *J. Am. Chem. Soc.*, 2016, **138**, 12328–12331.
6 M. E. McFadden and M. J. Robb, *J. Am. Chem. Soc.*, 2019, **141**, 11388–11392.
7 B. A. Versaw, M. E. McFadden, C. C. Husic and M. J. Robb, *Chem. Sci.*, 2020, **11**, 4525–4530.
8 M. E. McFadden and M. J. Robb, *J. Am. Chem. Soc.*, 2021, **143**, 7925–7929.
9 Z. Wang, Z. Ma, Y. Wang, Z. Xu, Y. Luo, Y. Wei and X. Jia, *Adv. Mater.*, 2015, **27**, 6469–6474.
10 Y. Lin, M. H. Barbee, C.-C. Chang and S. L. Craig, *J. Am. Chem. Soc.*, 2018, **140**, 15969–15975.
11 G. R. Gossweiler, G. B. Hewage, G. Soriano, Q. Wang, G. W. Welshofer, X. Zhao and S. L. Craig, *ACS Macro Lett.*, 2014, **3**, 216–219.
12 F. Verstraeten, R. Göstl and R. P. Sijbesma, *Chem. Commun.*, 2016, **52**, 8608–8611.
13 T. Kosuge, X. Zhu, V. M. Lau, D. Aoki, T. J. Martinez, J. S. Moore and H. Otsuka, *J. Am. Chem. Soc.*, 2019, **141**, 1898–1902.
14 K. Imato, A. Irie, T. Kosuge, T. Ohishi, M. Nishihara, A. Takahara and H. Otsuka, *Angew. Chem., Int. Ed.*, 2015, **54**, 6168–6172.
15 T. Wang, N. Zhang, J. Dai, Z. Li, W. Bai and R. Bai, *ACS Appl. Mater. Interfaces*, 2017, **9**, 11874–11881.
16 T. Sumi, R. Goseki and H. Otsuka, *Chem. Commun.*, 2017, **53**, 11885–11888.
17 Y. Lu, H. Sugita, K. Mikami, D. Aoki and H. Otsuka, *J. Am. Chem. Soc.*, 2021, **143**, 17744–17750.

18 S. Kato, S. Furukawa, D. Aoki, R. Goseki, K. Oikawa, K. Tsuchiya, N. Shimada, A. Maruyama, K. Numata and H. Otsuka, *Nat. Commun.*, 2021, **12**, 126.
19 J. Kida, K. Imato, R. Goseki, D. Aoki, M. Morimoto and H. Otsuka, *Nat. Commun.*, 2018, **9**, 3504.
20 S. Kato, K. Ishizuki, D. Aoki, R. Goseki and H. Otsuka, *ACS Macro Lett.*, 2018, **7**, 1087–1091.
21 Z. S. Kean, G. R. Gossweiler, T. B. Kouznetsova, G. B. Hewage and S. L. Craig, *Chem. Commun.*, 2015, **51**, 9157–9160.
22 J. M. Clough, J. van der Gucht and R. P. Sijbesma, *Macromolecules*, 2017, **50**, 2043–2053.
23 Z. Chen, J. A. M. Mercer, X. Zhu, J. A. H. Romaniuk, R. Pfattner, L. Cegelski, T. J. Martinez, N. Z. Burns and Y. Xia, *Science*, 2017, **357**, 475–479.
24 Y. Chen, A. J. H. Spiering, S. Karthikeyan, G. W. M. Peters, E. W. Meijer and R. P. Sijbesma, *Nat. Chem.*, 2012, **4**, 559–562.
25 R. Göstl and R. P. Sijbesma, *Chem. Sci.*, 2016, **7**, 370–375.
26 C. Baumann, M. Stratigaki, S. P. Centeno and R. Göstl, *Angew. Chem., Int. Ed.*, 2021, **60**, 13287–13293.
27 J. Yang, M. Horst, S. H. Werby, L. Cegelski, N. Z. Burns and Y. Xia, *J. Am. Chem. Soc.*, 2020, **142**, 14619–14626.
28 J. Yang, M. Horst, J. A. H. Romaniuk, Z. Jin, L. Cegelski and Y. Xia, *J. Am. Chem. Soc.*, 2019, **141**, 6479–6483.
29 J. R. Hemmer, C. Rader, B. D. Wilts, C. Weder and J. A. Berrocal, *J. Am. Chem. Soc.*, 2021, **143**, 18859–18863.
30 M. Karman, E. Verde-Sesto, C. Weder and Y. C. Simon, *ACS Macro Lett.*, 2018, **7**, 1099–1104.
31 M. Karman, E. Verde-Sesto and C. Weder, *ACS Macro Lett.*, 2018, **7**, 1028–1033.
32 Y. Pan, H. Zhang, P. Xu, Y. Tian, C. Wang, S. Xiang, R. Boulatov and W. Weng, *Angew. Chem., Int. Ed.*, 2020, **59**, 21980–21985.
33 H. Qian, N. S. Purwanto, D. G. Ivanoff, A. J. Halmes, N. R. Sottos and J. S. Moore, *Chem*, 2021, **7**, 1080–1091.
34 T. Muramatsu, Y. Okado, H. Traeger, S. Schrettl, N. Tamaoki, C. Weder and Y. Sagara, *J. Am. Chem. Soc.*, 2021, **143**, 9884–9892.
35 Y. Sagara, M. Karman, A. Seki, M. Pannipara, N. Tamaoki and C. Weder, *ACS Cent. Sci.*, 2019, **5**, 874–881.
36 T. Muramatsu, Y. Sagara, H. Traeger, N. Tamaoki and C. Weder, *ACS Appl. Mater. Interfaces*, 2019, **11**, 24571–24576.
37 Y. Sagara, M. Karman, E. Verde-Sesto, K. Matsuo, Y. Kim, N. Tamaoki and C. Weder, *J. Am. Chem. Soc.*, 2018, **140**, 1584–1587.
38 R. Sandoval-Torrientes, T. Carr and G. De Bo, *Macromol. Rapid Commun.*, 2021, **42**, 2000447.
39 Y. Sagara, H. Traeger, J. Li, Y. Okado, S. Schrettl, N. Tamaoki and C. Weder, *J. Am. Chem. Soc.*, 2021, **143**, 5519–5525.
40 S. Thazhathethil, T. Muramatsu, N. Tamaoki, C. Weder and Y. Sagara, *Angew. Chem., Int. Ed.*, 2022, **61**, e202209225.
41 H. Traeger, Y. Sagara, D. J. Kiebala, S. Schrettl and C. Weder, *Angew. Chem., Int. Ed.*, 2021, **60**, 16191–16199.
42 H. Traeger, Y. Sagara, J. A. Berrocal, S. Schrettl and C. Weder, *Polym. Chem.*, 2022, **13**, 2860–2869.
43 K. Imato, R. Yamanaka, H. Nakajima and N. Takeda, *Chem. Commun.*, 2020, **56**, 7937–7940.
44 Q. Verolet, A. Rosspeintner, S. Soleimanpour, N. Sakai, E. Vauthey and S. Matile, *J. Am. Chem. Soc.*, 2015, **137**, 15644–15647.
45 A. Colom, E. Derivery, S. Soleimanpour, C. Tomba, M. D. Molin, N. Sakai, M. González-Gaitán, S. Matile and A. Roux, *Nat. Chem.*, 2018, **10**, 1118–1125.
46 J. García-Calvo, J. Maillard, I. Fureraj, K. Strakova, A. Colom, V. Mercier, A. Roux, E. Vauthey, N. Sakai, A. Fürstenberg and S. Matile, *J. Am. Chem. Soc.*, 2020, **142**, 12034–12038.
47 A. E. Früh, F. Artoni, R. Brighenti and E. Dalcanale, *Chem. Mater.*, 2017, **29**, 7450–7457.
48 G. A. Filonenko and J. R. Khusnutdinova, *Adv. Mater.*, 2017, 1700563.
49 G. A. Filonenko, D. Sun, M. Weber, C. Müller and E. A. Pidko, *J. Am. Chem. Soc.*, 2019, **141**, 9687–9692.
50 G. A. Filonenko, J. A. M. Lugger, C. Liu, E. P. A. van Heeswijk, M. M. R. M. Hendrix, M. Weber, C. Müller, E. J. M. Hensen, R. P. Sijbesma and E. A. Pidko, *Angew. Chem., Int. Ed.*, 2018, **57**, 16385–16390.
51 T. Yamakado and S. Saito, *J. Am. Chem. Soc.*, 2022, **144**, 2804–2815.
52 R. Kotani, S. Yokoyama, S. Nobusue, S. Yamaguchi, A. Osuka, H. Yabu and S. Saito, *Nat. Commun.*, 2022, **13**, 303.
53 Y. Goto, S. Omagari, R. Sato, T. Yamakado, R. Achiwa, N. Dey, K. Suga, M. Vacha and S. Saito, *J. Am. Chem. Soc.*, 2021, **143**, 14306–14313.
54 M. Raisch, W. Maftuhin, M. Walter and M. Sommer, *Nat. Commun.*, 2021, **12**, 4243.
55 M. Taki, T. Yamashita, K. Yatabe and V. Vogel, *Soft Matter*, 2019, **15**, 9388–9393.
56 H. Hu, X. Cheng, Z. Ma, R. P. Sijbesma and Z. Ma, *J. Am. Chem. Soc.*, 2022, **144**, 9971–9979.
57 M. Zhang and G. De Bo, *J. Am. Chem. Soc.*, 2019, **141**, 15879–15883.
58 M. Zhang and G. De Bo, *J. Am. Chem. Soc.*, 2018, **140**, 12724–12727.
59 G. De Bo, *Chem. Sci.*, 2018, **9**, 15–21.
60 B. Brough, B. H. Northrop, J. J. Schmidt, H.-R. Tseng, K. N. Houk, J. F. Stoddart and C.-M. Ho, *Proc. Natl. Acad. Sci. U. S. A.*, 2006, **103**, 8583–8588.
61 A. Dunlop, J. Wattoom, E. A. Hasan, T. Cosgrove and A. N. Round, *Nanotechnology*, 2008, **19**, 345706.
62 S. Du, H. Fu, X. Shao, C. Chipot and W. Cai, *J. Phys. Chem. C*, 2018, **122**, 9229–9234.
63 Z. Wu, S. Wang, Z. Zhang, Y. Zhang, Y. Yin, H. Shi and S. Jiao, *RSC Adv.*, 2022, **12**, 30495–30500.
64 Y. Sagara, T. Komatsu, T. Ueno, K. Hanaoka, T. Kato and T. Nagano, *J. Am. Chem. Soc.*, 2014, **136**, 4273–4280.
65 A. Yoshizawa and M. Inouye, *ChemPhotoChem*, 2018, **2**, 353–356.
66 H. Maeda, T. Maeda, K. Mizuno, K. Fujimoto, H. Shimizu and M. Inouye, *Chem. – Eur. J.*, 2006, **12**, 824–831.
67 S. Amemori, K. Kokado and K. Sada, *Angew. Chem., Int. Ed.*, 2013, **52**, 4174–4178.
68 S. B. Krishnan, R. Krishnan and K. R. Gopidas, *Chem. – Eur. J.*, 2018, **24**, 11451–11460.
69 Q. Wang, T. R. Chan, R. Hilgraf, V. V. Fokin, K. B. Sharpless and M. G. Finn, *J. Am. Chem. Soc.*, 2003, **125**, 3192–3193.
70 V. V. Rostovtsev, L. G. Green, V. V. Fokin and K. B. Sharpless, *Angew. Chem., Int. Ed.*, 2002, **41**, 2596–2599.